ELSEVIER

Chemical Geology 177 (2001) 187–200

CHEMICAL GEOLOGY
INCLUDING
ISOTOPE GEOSCIENCE

www.elsevier.com/locate/chemgeo

White Island volcano, New Zealand: carbon dioxide and sulfur dioxide emission rates and melt inclusion studies

Lois J. Wardell [a,*], Philip R. Kyle [a,b], Nelia Dunbar [b], Bruce Christenson [c]

[a] *Department of Earth and Environmental Science, New Mexico Institute of Mining and Technology, 801 Leroy Place, Socorro, NM 87801-4796, USA*

[b] *New Mexico Bureau of Mines and Mineral Resources, New Mexico Institute of Mining and Technology, 801 Leroy Place, Socorro, NM 87801-4796, USA*

[c] *Institute of Geological and Nuclear Sciences, Wairakei, New Zealand*

Received 17 February 2000; accepted 10 June 2000

Abstract

CO_2 and SO_2 emission rates are reported for the volcanic gas plume from White Island, the most active volcano in New Zealand. SO_2 emission rates were measured 16 times by correlation spectrometer (COSPEC) from 1986 to 1999 and range from 171 to 900 Mg day^{-1}. We estimate the average SO_2 emission rate was 430 ± 70 Mg day^{-1} between 1983 and 1999. CO_2 emission rates of 2570 and 2650 Mg day^{-1} were determined in January 1998 by aircraft directly in the plume using a CO_2 analyzer and a ladder survey technique. Using the average SO_2 emission rate and a CO_2/S weight ratio of 3.6 previously reported for fumarole samples collected from the crater floor, an indirect estimate of the CO_2 is 1550 Mg day^{-1}.

A soil gas survey of CO_2 emissions from the crater floor gave an emission rate of 8.7 Mg day^{-1}. Soil gases contribute less than 1% of the total CO_2 emitted from this volcano and show that the magmatic degassing of the underlying andesite magma is mostly isolated to the active crater and associated fumaroles.

Volatile elements (H_2O, Cl, F, S) were measured in melt inclusions trapped in plagioclase and clinopyroxene crystals. The low H_2O contents (0.6 ± 0.2 wt.%) of melt inclusions suggest that crystal formation occurs at pressures of 35 to 70 bars. The Cl contents of melt inclusions (0.10–0.18 wt.%) are higher than that of matrix glass (0.11 wt.%), suggesting Cl was lost from the magma between the time of crystallization and eruption. Therefore, Cl degassing also occurred in part at shallow depths in the magmatic system. The low SO_2 contents of both melt inclusions and matrix glass implies that it exsolves at depths greater than 300 m. CO_2 is insoluble in andesitic magma and probably was degassing with SO_2 at depths > 300 m within the magmatic system.

Keywords: White Island; Carbon dioxide; Sulfur dioxide; Melt inclusions; COSPEC

1. Introduction

White Island is an andesitic composite volcano located 50 km off the coast of the North Island at the northeastern end of the Taupo Volcanic Zone. It is

* Corresponding author. Tel.: +1-505-835-5994; fax: +1-505-835-6436.

E-mail address: wardell@nmt.edu (L.J. Wardell).

0009-2541/01/$ - see front matter
PII: S0009-2541(00)00391-0

the most frequently active volcano in New Zealand with numerous small eruptions recorded during the past 150 years (Cole and Nairn, 1975; Simkin and Siebert, 1994). The volcano has undergone a series of eruptive cycles since 1976 (Houghton and Nairn, 1989). The crater floor is lined with fumaroles and acid lakes are a transient feature in the deepest areas of the crater floor. The crater is underlain by an acidic hydrothermal system that remains isolated from the seawater by chemically sealed zones (Giggenbach and Sheppard, 1989; Giggenbach, 1987, 1992; Hedenquist et al., 1993). Because of the ease of access and the generally mild activity, White Island has been the focus of many volcanological studies. A significant number of the studies of the volcanic activity have been surveillance orientated in nature and have attempted to predict future eruptive activity.

In this paper, we report CO_2 and SO_2 emission rates and volatile contents of melt inclusions and matrix glass from recent ejecta. These provide a picture of the degassing character of this continuously erupting volcano. SO_2 emission rates were collected over a 14-year period, giving a better estimate of the average long-term SO_2 emission rate. This has a direct effect upon the flux rate estimates of other volatile species as they are based upon the SO_2 emission rate. White Island has been viewed as a present-day analog for Cu–Au ore depositing systems (Hedenquist et al., 1993). This, and similar flux models for the volcano (e.g., Marty and Giggenbach, 1990), have relied on a few COSPEC measurements of SO_2 emissions rates reported by Rose et al. (1986).

The CO_2 emission rates we are reporting are the first direct airborne measurements of CO_2 for this volcano and the results show White Island's significance as a contributor of volcanic CO_2. Due to the low solubility of CO_2 in magmatic melts, it is completely exsolved from the parent magma by the time it reaches the surface. Thus, variations in gas species relative to CO_2 are likely to reflect processes affecting that species rather than the CO_2 (Giggenbach, 1996). The emission rates of SO_2 and CO_2 can be useful as a predictive tool for eruptive behavior as they reflect changes deeper within the system and analysis of melt inclusions assist in constraining the degassing behavior.

Melt inclusions provide insight into the volatile history of a magma, and thus compliment the study of magmatic degassing. Volatiles are lost from a magma by degassing or during eruptions, thus leaving no direct method to determine the pre-eruptive volatile contents of the magma. Because melt inclusions are trapped and often quenched within phenocrysts, they can indicate the magmatic volatile composition at the time of entrapment (e.g., Roedder, 1984). By comparing the volatile contents of melt inclusions and degassed magma (matrix glass from explosive ejecta), it is possible to assess changes in magmatic volatile contents resulting from volcanic eruptions (Devine et al., 1984; Palais and Sigurdsson, 1989).

2. Analytical methods

2.1. Airborne CO_2 flux measurements

The CO_2 flux measurements were determined by measuring the CO_2 concentration in the plume while flying airborne transects through a perpendicular cross-section of the plume, similar to the method described by Gerlach et al. (1997). We used a LI-COR, model LI-6262 CO_2 analyzer interfaced to a Hewlett-Packard 200LX Palmtop for data acquisition and recorded real time concentrations at 1-s intervals. The LI-COR analyzer was calibrated using 0 and 2000 ppm CO_2 gas standards. The analyzer was equipped with factory-installed temperature and pressure transducers to yield real-time absolute CO_2 concentrations in μmol/mol. A flow control unit precedes the analyzer as the LI-COR is calibrated at a specific flow rate. The LI-COR analyzer has a reported accuracy of ± 1 ppm. The aircraft position was determined every 2 s using a Garmin 12XL GPS unit and recorded on an interfaced laptop computer. Although the GPS unit gave acceptable horizontal locations (latitude and longitude) there were greater errors in the altitude. Therefore, the aircraft altitude was manually recorded from the aircraft barometric altimeter and substituted for the GPS altitude values.

Data from the LI-COR and GPS were combined and reduced into a spreadsheet. The ambient CO_2 concentration was measured along the flight path to the island and subtracted out from the values mea-

sured in the plume to give a volcanic CO_2 concentration. A contour plot was constructed of the CO_2 concentration in the plume cross-section normal to the wind direction. SURFER (Golden Software, Golden, CO) software was employed for the contour plot using kriging algorithms. From the contour plot, the CO_2 concentration per unit area was determined and multiplied by the wind speed to yield a flux rate. Error for this method was evaluated by Koepenick et al. (1996) by applying this method to known emissions from a coal-burning power plant. CO_2 emission rates could be measured within $\pm 10\%$ at 1 and 2 km from the plant. Our measurements at White Island were within 1 km of the crater. When this method was applied at Popocatepetl volcano by Gerlach et al. (1997), an error of $\pm 20\%$ for a 95% confidence interval was calculated, with the natural variance of wind speed being the largest source of random error.

2.2. Soil gas CO_2 emissions

CO_2 soil gas flux measurements were made using the accumulation chamber method described by Norman et al. (1992). A 9.56-l aluminum box containing a small fan to provide circulation was placed open-side-down on the ground. CO_2 build-up in the accumulation box was monitored by circulating the enclosed air through the LI-COR CO_2 analyzer and back into the box. The rate of accumulation inside the box was determined from the slope (dx/dt) of the plot of time vs. concentration. The initial CO_2 concentration inside the box was not scrubbed below ambient. Flux was then calculated by employing the ideal gas law in the equation,

$$CO_2\ \text{FLUX} = \frac{\frac{PV}{RT} \cdot \frac{dx}{dt}}{A}$$

where P is the ambient pressure in atmospheres; V is the volume of the accumulation box; A is the footprint area of the accumulation box; R is the natural gas constant; T is the ambient temperature; dx/dt is the slope from a plot of concentration vs. time.

Time series of the CO_2 concentration in the box determines the flux in units of g m^{-2} s^{-1}. Error for the accumulation chamber method as evaluated by laboratory experiments, is reported at $\pm 10\%$ by Gerlach et al. (1998) and $\pm 15\%$ by Chiondini et al. (1998).

2.3. SO_2 emission rates

SO_2 emission rates were measured using Barringer correlation spectrometers (COSPEC V). Measurements were made by standard airborne techniques (Stoiber et al., 1983) except on 12 January 1987 when the plume was scanned by traversing under the plume in a boat with the COSPEC aimed vertically upward. From 1983 until 1992, wind speeds were estimated using ground observations (mainly from fishermen in the vicinity of the island) and from ground and radiosonde measurements made at the nearest cities of Whakatane and Rotorua. Since 1992, wind speeds were measured at plume level using differences between indicated airspeed and the ground speed as measured by GPS instrumentation.

2.4. Melt inclusions

Crystals and matrix glass were separated from a scoria block erupted in March 1989 (collected by W. Giggenbach). The phenocrysts and associated matrix glass (either free scoriaceous glass or glass adhering to phenocrysts) were analyzed for major elements, Cl, and S using a Cameca SX-100 electron microprobe at N. M. Institute of Mining and Technology. Prior to analysis the samples were examined by backscattered electron imaging. A 10-nA beam current and beam diameters of 15, 20, or 25 μm were used for glass analyses. Count times were 20 s except for Na (40 s), Cl (30 s) and S (60 s). For feldspar and pyroxene, a beam current of 20 nA, and beam size of 10 and 1 μm, respectively, were used. ZAF matrix correction techniques were used for data reduction. Errors based on replicate analyses of reference materials (glasses KE-12 and KN-18, Devine et al., 1984) and counting statistics are cited in Table 1.

Ion microprobe analyses were made on a Cameca IMS 3f ion microprobe at Arizona State University (Hervig et al., 1989). A 1- to 2-nA mass-analyzed primary beam of $^{16}O^-$ ions was focused to 10–20 μm in diameter. Secondary ions were accelerated to $+4500$ eV and the transfer optics and field aperture

Table 1
Average or range of major, volatile and trace element abundances of melt inclusions, matrix glass and phenocrysts from White island explosive ejecta

	Melt inclusions	Matrix glass		Phenocrysts		
		Crystalline	Non-crystalline	Feldspar	Cpx	Opx
SiO_2 (wt.%)	59.70–66.40	65.10	63.89	52.62	52.37	53.09
TiO_2 (wt.%)	0.74–2.21	1.10	1.08		0.42	0.28
Al_2O_3 (wt.%)	12.89–14.27	13.75	14.07	29.22	1.70	1.14
MgO (wt.%)	1.06–3.11	1.54	1.84		16.35	26.03
CaO (wt.%)	4.22–5.43	4.32	4.88	12.64	18.53	2.05
MnO (wt.%)	0.02–0.19	0.06	0.05		0.29	0.35
FeO (wt.%)	6.01–8.50	6.49	6.12	0.89	10.08	16.83
Na_2O (wt.%)	2.92–3.64	3.38	3.46	3.83	0.36	0.03
K_2O (wt.%)	2.80–3.29	3.22	2.96	0.38	0.03	0.02
P_2O_5 (wt.%)	0.08–0.45	0.17	0.17			
H_2O (wt.%)	0.6 (0.2)	0.3 (0.2)				
SO_2 (wt.%)	0.02 (0.01)	0.01 (0.01)	0.01 (0.01)			
Cl (wt.%)	0.101–0.177	0.112 (0.018)	0.113 (0.001)			
Li (ppm)	35 (7)	26 (6)			3	
B (ppm)	50 (7)	53 (7)			6	
Rb (ppm)	79 (11)	83 (12)			19	
Y (ppm)	23 (3)	23 (2)			7	
Sr (ppm)	118 (11)	119 (18)			0	
Zr (ppm)	181 (27)	186 (15)			4	
Nb (ppm)	5 (1)	5 (1)			0	
Cs (ppm)	8 (3)	10 (2)			5	
Ba (ppm)	1020 (100)	1059 (140)			1	
Ce (ppm)	31 (8)	29 (6)			0	
Th (ppm)	3 (3)	2 (3)			0	
n (Electron probe)	24	15	4	8	1	1
n (Ion probe)	9	3			1	

Major elements (Cl and S) were analyzed by electron microprobe: all other analyses were made by ion microprobe. Errors of determination for the electron microprobe, based on replicate analyses or reference materials and counting statistics (in wt.%): SiO_2 ± 0.5, TiO_2 ± 0.01, Al_2O_3 ± 0.03, MgO ± 0.12, CaO ± 0.05; MnO ± 0.03, FeO ± 0.07, Na_2O ± 0.09, K_2O ± 0.19, P_2O_5 ± 0.1. Errors for Cl and S, based on replicate analyses of a standard, are both around ± 100 ppm. Ion microprobe errors are ± 0.1 wt.% for H_2O, and $\pm 15\%$ for other elements. Standard deviations for sets of ion microprobe analyses and electron microprobe analysis of Cl and S are shown in parentheses.

were set to accept secondary ions into the mass spectrometer from a 20-μm circular area on the sample. After the secondary ion signal had stabilized the sample voltage was ramped ± 100 V from 4500 while the intensity of $^{30}Si^+$ was monitored. The sample voltage was returned to the centroid of the intensity vs. sample potential curve to correct for the small amount of charging which occurred. The energy bandpass was fully open (130 eV) for early analyses, but in the later stages of this study we closed it to 40 eV. Molecular interferences were removed by collecting secondary ion intensities at high energies, which were achieved by offsetting the sample voltage -75 V from the centroid position for H, Li, B, F, P, Ti, Fe, Rb, Sr, Y, Zr, Nb, Cs, Ba, Ce and Th.

The secondary ion intensity for hydrogen was calibrated using experimentally hydrated rhyolitic glasses analyzed by infrared spectroscopy (kindly provided by E. Stolper). Trace elements were calibrated against NBS 610, a sodium- and silica-rich glass containing nominally 500 ppm of 61 trace elements. Comparison of NBS-610 with several bulk-analyzed rhyolitic glasses indicated that the trace elements studied were within 10% of their nominal concentration. Exceptions are P, and Ti, which were

present at levels of 350 and 590 ppm, respectively. Analyses use the corrected value for NBS-610. Observed reproducibility of secondary standards suggested that the precision of analyses are: Li, B, Rb, Y, Zr, Nb, Ce and Th $\pm 10\%$, P $\pm 25\%$, Ba, Sr $\pm 25\%$. Reproducibility of the analyses for H_2O is no worse than ± 0.5 wt.%, and is usually better.

3. Results

3.1. Airborne CO_2 flux measurements

Two measurements were made on 2 January 1998, using a single-engine Cessna 172 aircraft. The intake line for the CO_2 analyzer was fixed to the left wing strut of the aircraft well away from any exhaust from the engine. For the two plume flights, 9 and 12 passes were made through the plume, most at $\sim$ 30-m vertical increments and normal to the plume and wind direction. Aircraft speed was kept at 40 m/s. A wind speed of 3 m/s was measured using GPS.

Ambient CO_2 levels were difficult to ascertain as the variation in atmospheric concentrations outside of the plume ranged by 5 ppm. The variations in background levels changed with the time of day and with the altitude and position upwind from the crater structure. A conservative estimate of the ambient CO_2 concentration was selected for each flight by choosing the highest observed value observed outside the plume. The CO_2 concentrations in the plume were as high as 6 ppm above the highest ambient background value.

The first flight had an ambient atmospheric CO_2 of 350 ppm. Based on contour plots of the CO_2 concentration of the plume cross-section, the total flux was calculated to be 2570 Mg day^{-1}. The second flight, performed later in the afternoon yielded a CO_2 flux of 2650 Mg day^{-1} with a background level of CO_2 at 353 ppm. Based on the contour configurations (Fig. 1), it appears that small sections of the plume may have escaped the airborne transects.

3.2. Soil gas CO_2 emissions

Nineteen soil gas flux values were measured on the crater floor (Fig. 2) on 01 January 1998, the day prior to the airborne plume measurements. Sample locations were dispersed over the crater floor without

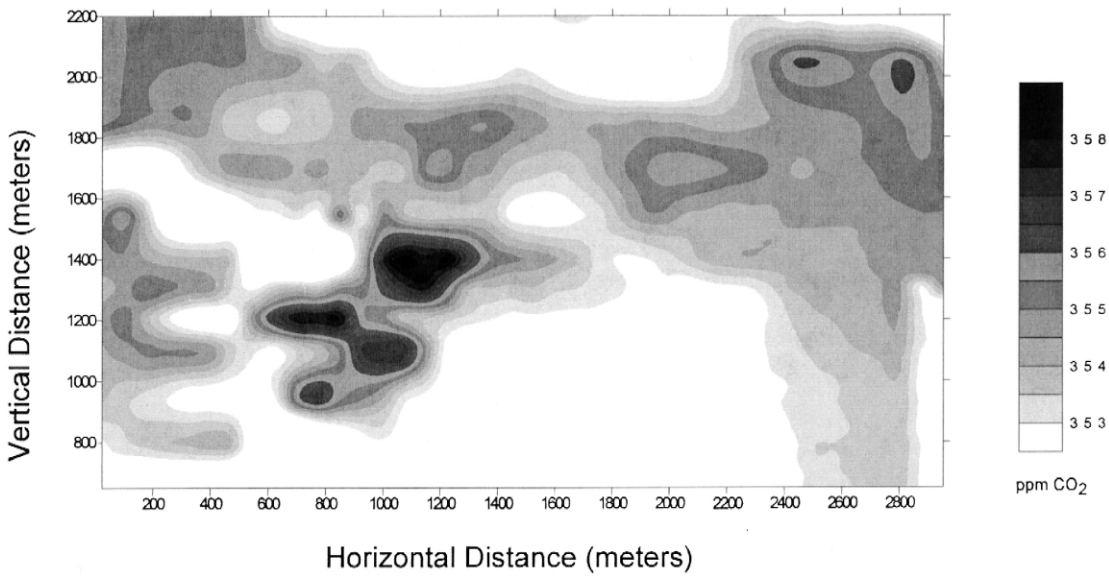

Fig. 1. CO_2 concentrations of the plume cross-section at White Island. The main axis of the plume was directed to the southwest. This contour plot was constructed in SURFER software by pairing CO_2 concentrations with GPS locations taken at 1-s intervals during the flight through the plume transects. The scale for the contours shows CO_2 concentrations in ppm.

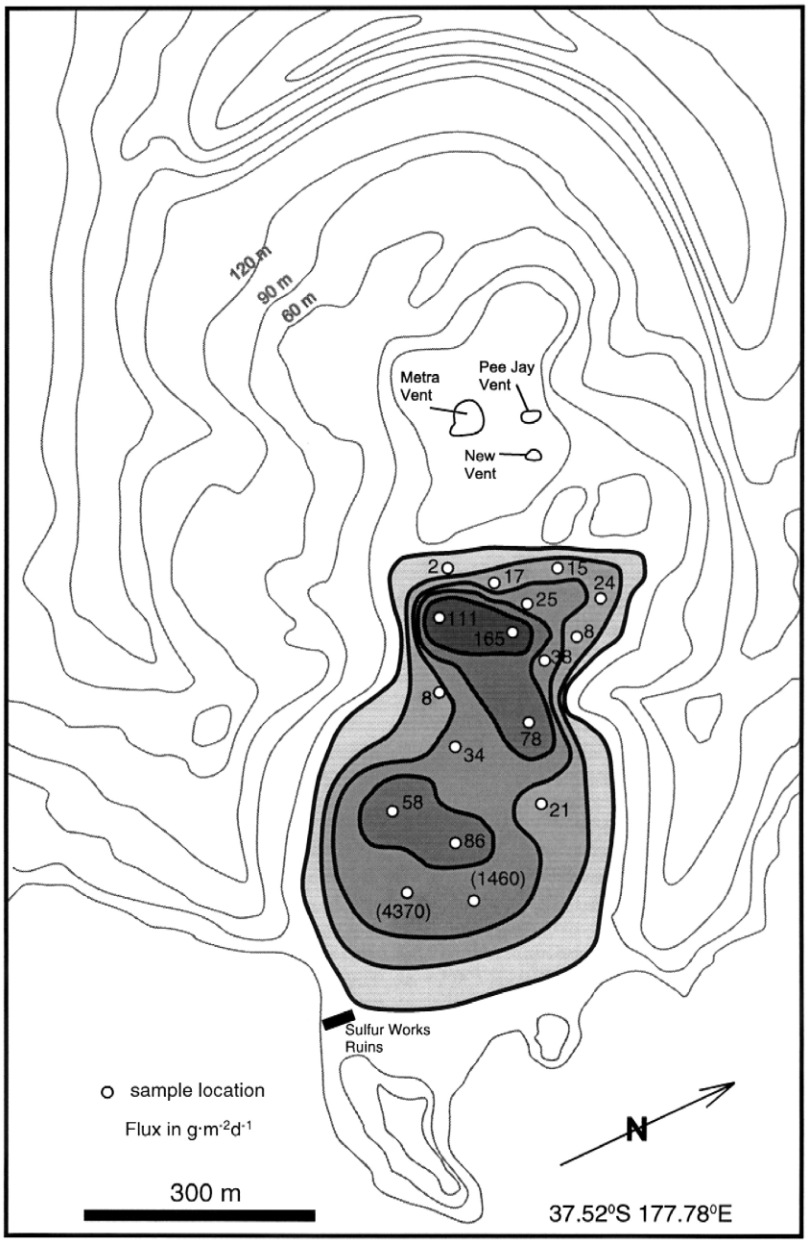

Fig. 2. Contour map of CO_2 soil gas concentrations on the crater floor of White Island. The shaded area of the map is the crater floor and shows the contours derived from soil gas flux rates in g m^{-2} day^{-1}. The vents labeled above the shaded crater floor show the location of the main crater where the volcanic plume originates. Values in parentheses are anomalies near thermal springs.

using a grid and included a variety of topographic features. Values ranged from 2 g m^{-2} day^{-1} on hard soil to 4370 g m^{-2} day^{-1} near a thermal spring. The data were plotted and contoured using SURFER software. The anonymously high CO_2 values near the thermal spring were not included in the contour

plot but considered separately as this small area would have biased the contours. A total soil flux of 8.7 mg day^{-1} was calculated for the crater floor using SURFER which included an area of 200,000 m^2. Not included in the calculations were visible areas of active degassing such as the fumaroles, which are found along the edges of the crater floor, and active underwater seeps. Due to the difficult terrain and limited scope of this project, soil gas measurements excluded surveying the outer flanks of the crater for any zones of CO_2 emissions. Since only a limited part of the passive degassing was evaluated, the contribution of volcanic CO_2 by non-plume sources for this island volcano cannot be established by this study.

3.3. SO_2 emission rates

The SO_2 emission rates measured by COSPEC are given in Table 2 and for this study range from 171 Mg day^{-1} to a single measurement of 926 mg day^{-1}. On 17 May 1992, just as aircraft passes beneath the plume were being completed, a small eruption occurred sending an ash plume to an altitude of about 1500 m. The leading edge of the wind-driven plume passed directly over the aircraft and we were able to get a COSPEC measurement of 926 Mg day^{-1}. It was likely that the denser parts of the eruption cloud were significantly higher in SO_2 as the measurement was made under a segment of the plume which was only about a third as wide as the main plume. The highest recorded value of 1230 Mg day^{-1} reported by Rose et al. (1986) occurred prior to an eruptive episode.

For the period of December 1983 till May 1992, the average SO_2 flux was 650 Mg day^{-1}. There appears to be a decrease in the emission rate from 1993 through the early half of 1998 (Table 2) and the average SO_2 flux value for 1993 through 1999 is 300 Mg day^{-1}. The overall reported average from the 17-year database of COSPEC measurements is 430 ± 70 Mg day^{-1}.

Table 2
SO_2 emission rates measured by correlation spectrometer (COSPEC) at White Island, New Zealand

Date	Number of scans	SO_2 flux (Mg day^{-1})
23 December 1983	7	1230 ± 300[a]
21 November 1984	7	320 ± 120[a]
7 January 1985	5	350 ± 150[a]
7 February 1986	10	570 ± 100
12 January 1987	3	830 ± 200
4 November 1987	8	900 ± 100
14 December 1990	7	362 ± 80
17 May 1992	7	350 ± 50
17 May 1992	1	926
8 December 1993	7	171 ± 26
8 March 1994	5	259 ± 27
16 August 1995	5	187 ± 20
15 November 1995	5	314 ± 78
26 April 1996	9	180 ± 54
18 October 1996	5	298 ± 126
20 March 1998	7	195 ± 66
3 April 1998	10	373 ± 125
11 September 1998	12	891 ± 404
9 December 1998	11	239 ± 127
23 January 1999	12	215 ± 72
Mean		433 ± 70

[a] Data from Rose et al. (1986).

3.4. Melt inclusions

Plagioclase and pyroxene phenocrysts contain abundant, light to dark brown, mainly bubble-free melt inclusions. The melt inclusions are most common in plagioclase cores. Backscattered electron imaging shows that the cores of some plagioclase have a "spongy" texture (Fig. 3A), similar to cores of anorthoclase crystals from Mt. Erebus, Antarctica (Dunbar et al., 1994). Melt inclusions are mainly 5–40 μm but may reach 100 μm. Some melt inclusions are cracked and those adhered to the walls of the host crystal show shrinkage voids formed during cooling (Fig. 3B). Analyses were made of the various melt inclusions to examine systematic differences due to size, morphology, location with a crystal and the degree of cracking.

Vesicular matrix glass adhering to crystals was analyzed. The matrix glass is typically partially crystalline, containing small microlites of feldspar and pyroxene (Fig. 3B). Non-crystalline glass also occurs mainly in interstices in glomeroporphyritic clumps of plagioclase and pyroxene. Nucleation of microlites was apparently inhibited in this interstitial glass.

A total of 24 melt inclusions were analyzed (Table 1). Most have dacite compositions (following the

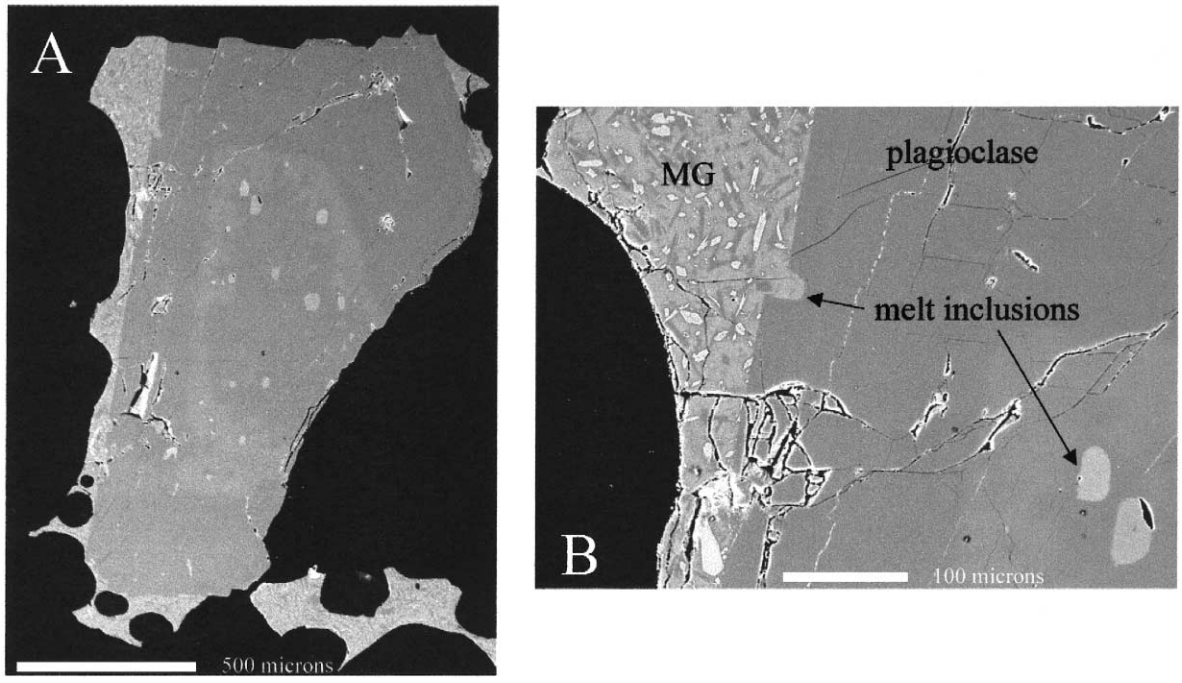

Fig. 3. Backscattered electron images of a plagioclase feldspar crystal from a 1989 White Island eruption. Panel (A) shows the core (outlined by a light band) and rim of the crystal, melt inclusions distributed throughout the crystal, but more concentrated in the crystal core, and matrix adhering to the outside of the crystal. Panel (B) shows the crystalline nature of the matrix glass (MG) adhered to the outside of the plagioclase crystal. Dark grey areas in matrix material are plagioclase, the medium grey shade is glass, and the lightest areas are pyroxene crystals. A melt inclusion, in the process of formation, is also visible.

classification of Cox et al., 1979) although inclusions in the spongy plagioclase cores are andesite. Both the andesite and dacite compositions are similar to analyzed rocks samples from White Island (Clark et al., 1979). The melt inclusions show systematic chemical compositions (Fig. 4). Inclusions from the centers of crystals are more basic than those from the outer areas of crystals. There is some overlap between the two populations. Inclusions from the center of crystals are higher in TiO_2, FeO, MgO, P_2O_5, and Cl and lower in SiO_2, K_2O and Al_2O_3 than those from the crystal rims. Melt inclusions in an orthopyroxene crystal, and in a plagioclase but in contact with an orthopyroxene crystal inclusion, contain significantly less MgO than other inclusions in plagioclase. It is likely that some post-entrapment crystallization (e.g., Watson, 1976) has occurred in pyroxene-hosted melt inclusions. The similar CaO and Al_2O_3 content of the inclusion trapped orthopyroxene and those found in plagioclase suggest that post-entrapment crystallization has not occurred in plagioclase-hosted inclusions.

Fifteen analyses were made of crystalline matrix glass and four of non-crystalline matrix glass (Table 1). Analysis of crystalline glass was difficulty because microlite-free areas of glass were hard to find. Similarities and differences in composition occur between the matrix glass and melt inclusions (Fig. 4). The crystalline matrix glass has lower MgO, CaO, and FeO than the melt inclusions. The crystallization of microlites is likely to be responsible for these chemical differences because MgO and FeO are compatible in pyroxene and CaO is compatible in both pyroxene and plagioclase. Therefore, the crystalline matrix glass composition reflects growth of these two phases. Non-crystalline matrix glass was

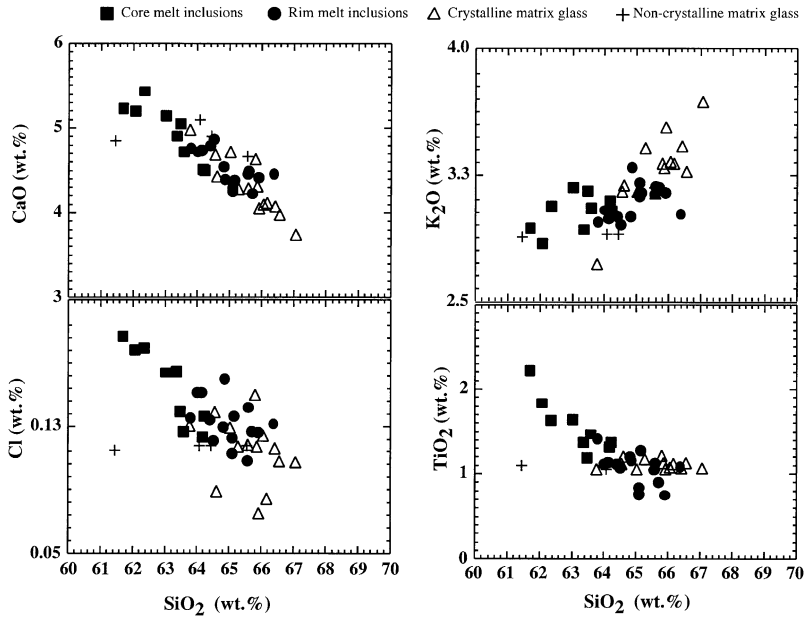

Fig. 4. SiO_2 vs. CaO, K_2O, Cl and TiO_2 in wt.% for melt inclusions from the cores and rims of plagioclase crystals, as well as crystalline and non-crystalline matrix material, as determined by electron microprobe analysis. The analytical errors are discussed in Table 1.

rare and only four analyses were made. Two of the analyses were of glass in a reentrant cavity in plagioclase and these are similar to the mean composition of melt inclusions. The other two analyses were made of glass in an interstitial area between a plagioclase and two pyroxene crystals. The composition of this glass appears to reflect crystallization of pyroxene following isolation of the glass in the interstitial area.

Volatile elements, H_2O, Cl, and SO_2 show some differences between melt inclusions and matrix glass but no differences occur between different sized inclusions, or between cracked and fractured inclusions. The H_2O and Cl abundances in melt inclusions are higher than that of matrix glass whereas the SO_2 concentrations are indistinguishable and low (100–200 ppm) (Table 1, Fig. 4). The Cl concentrations in melt inclusions from the centers of crystals are higher than those in crystal rims (Fig. 4), although the same trend is not observed for SO_2 concentrations. The SO_2 and Cl contents of crystalline and non-crystalline matrix glasses are indistinguishable.

Trace element abundances of melt inclusions and crystalline matrix are indistinguishable (Table 1).

4. Discussion

4.1. Airborne CO_2 flux measurements

Previously reported CO_2 flux values for White Island were based on the CO_2/S_t ratios from fumarole samples and an average SO_2 emission rate of 300–350 Mg day^{-1} reported by Rose et al. (1986) (Table 3). This method assumes that the fumarole samples are representative of the entire volcanic plume (Rose et al., 1986). Fumaroles are shallow surface features and tend to be more easily affected by hydrologic and shallow subsurface conditions (Giggenbach and Sheppard, 1989) and thus vary with temperature. As most of the gas in the volcanic plume is derived from high temperature fumaroles within the inaccessible crater, data from equivalent high temperature fumaroles are more applicable but

Table 3
Summary of CO_2 emission rates reported for White Island, New Zealand

Date	CO_2 flux (Mg day^{-1})	Method	References
2 January 1998	2570	Direct/LICOR	This study
2 January 1998	2650	Direct/LICOR	This study
1985–1992	1550	Gas Ratio/COSPEC	This study
1988	780[a]	Gas ratio/COSPEC	Giggenbach and Matsuo (1991)
1988	2040 (1080)[a]	Gas ratio/COSPEC	Tedesco and Toutain (1991)
1988	1400	Gas ratio/COSPEC	Marty and Giggenbach (1990)
1984–1985	1150–1260	Gas ratio/COSPEC	Giggenbach and Sheppard (1989)
1982–1984	900–1000	Gas ratio/COSPEC	Rose et al. (1986)

[a]Calculated from published data.

still are likely an unrepresentative hydrological variation.

The CO_2 flux estimate of 2040 Mg day^{-1} reported by Tedesco and Toutain (1991) is significantly higher than the 900–1000 Mg day^{-1} reported by Rose et al. (1986) and the 1150–1260 Mg day^{-1} of Giggenbach and Sheppard (1989) (Table 3). Tedesco and Toutain (1991) calculated their flux using the measured CO_2/SO_2 molar ratio in the fumarole samples rather than the CO_2/S_t weight ratio. Using a CO_2/S_t weight ratio calculated from Tedesco and Toutain (1991) yields a value of 1080 Mg day^{-1}, which is more consistent with the earlier flux rates. The three other flux values of 780, 2040 and 1400 Mg day^{-1} (Table 3) calculated in 1998 differ even though all were calculated using the same SO_2 flux and results from two fumarole analyses sampled during the IAVCEI workshop at White Island (Giggenbach and Matsuo, 1991; Tedesco and Toutain, 1991; Marty and Giggenbach, 1990). The differences resulted because different CO_2/S_t or CO_2/SO_2 ratios were used from two different fumaroles or an average of the two. In addition, this method employed COSPEC measurements done in November 1984 and January 1985 while sampling of the fumaroles were done in February 1988. The resultant CO_2 flux rate is not characteristic of the activity or conditions that were occurring in 1984/1985 or 1988. Although acquiring long-term averages of both the SO_2 flux and the CO_2/S_t ratio from fumaroles would yield an overall CO_2 flux value, it still may not be representative of the magnitude emitted from the plume.

The average CO_2 flux can be calculated using the average SO_2 flux of 430 Mg day^{-1} and an estimate of the CO_2/S_t in the plume. Most studies (Table 3) used a CO_2/S_t ratio of 3.6. This results in a CO_2 flux of 1550 Mg day^{-1}, which is somewhat less that what was observed with our airborne measurements. Therefore, higher values observed in the airborne study may indicate a higher rate of degassing or possibly a difference related to methodology or the level of activity during the measurement.

Volcanic CO_2 emission rates from volcanoes show a significant range (Table 4) although the number of volcanoes that have been measured are small. Flux values in Table 4 are taken from one or a few measurements and in some cases, crude estimates. These values do not reflect degassing variation or activity and in most cases, are the only reported CO_2 flux for the respected volcano. The CO_2 flux of 2600 Mg day^{-1} from White Island volcano is similar to that reported for Kilauea (Gerlach et al., 1997) but is significantly lower than more voluminously degassing volcanoes like Etna and Popocatépetl. Still, it is clear that White Island is a significant source of volcanic-derived CO_2 to the atmosphere.

4.2. Soil gas CO_2 emissions

Our results found that the soil gas emissions from the crater floor were less than 1% of the total CO_2 flux from the volcano's plume. Judging from the data summary in Table 4, there appears to be a large variability in the contribution of soil degassing from active volcanoes. Although the contribution of CO_2 from White Island's crater floor appears to be insignificant, the contribution from other non-plume sources were not evaluated. Therefore, CO_2 contributions from passive soil degassing and fumarole

Table 4
Comparison of White Island CO_2 emission rates with other volcanoes

	Flux (mg day^{-1})	% From soil	Source
Mt. Etna	70,000	10–50	Carbonnelle et al. (1985)
	11–38,000		Allard (1998)
Popocatépetl	6400	0	Gerlach et al. (1997), Varley (1998)
	40,000		Delgado et al. (1998)
Oldoinyo Lengai	7200	<2	Koepenick et al. (1996)
Augustine	6000	–	Symonds et al. (1992)
Mt. St. Helens	4800	–	Casadevall et al. (1983)
Stromboli	3000	–	Allard et al. (1994)
Kilauea	2800	~ 50	Gerlach and Graeber (1985), O'Keeffe (1994)
White Island	2600	<1	This paper
Mt. Erebus	1850	–	Wardell and Kyle (1999)
Redoubt	1800	–	Casadevall et al. (1990)
Grimsvotn	360	–	Brantley et al. (1993)
Vulcano	270	20	Carbonnelle et al. (1985)

sources cannot be considered insignificant by this study and further work is needed to quantify the emissions of this source.

4.3. SO_2 emission rates

COSPEC SO_2 emissions are important in that they allow emission rates of many other gas and aerosol species to be calculated. If the ratio of a gas or aerosol species to SO_2 can be determined from filters, gas samples, or airborne methods then the emission rate of that species can be determined using the COSPEC data. For these calculations, it is necessary to assume that the sulfur species emitted from the volcano are all oxidized to SO_2 in the atmosphere. In Section 4.1, we discussed indirect estimates of CO_2 emission based on the COSPEC data and CO_2/S_t determined directly in fumarole samples.

The SO_2 emission rates for White Island show some variability, which is undoubtedly related to the eruptive state of the volcano over the 17-year study period. Although the number of SO_2 flux measurements are small and were made infrequently, there is an increase in SO_2 during eruptive periods. The highest SO_2 flux of 1230 Mg day^{-1} was measured on 27 November 1983 and, as discussed by Rose et al. (1986), preceded a major eruption on 25 December 1983. Likewise, the 12 January 1987 SO_2 flux of 830 Mg day^{-1} was high and preceded a significant eruption on 25 January 1987. On the other hand, the 17 May 1992 eruption was very small and the SO_2 flux of 350 Mg day^{-1} measured just minutes prior to the eruption was not anomalous. An average long-term emission rate of ~ 430 Mg day^{-1} for White Island is fairly typical of passively degassing andesitic volcanoes (Andres and Kasgnoc, 1998).

The periodic eruption of primary andesitic bombs and ash are clear indications that andesitic magma is very close to the surface at White Island. Much of the variation in degassing rates of SO_2 are likely due to fluctuations in the supply of andesitic magma in the conduit underlying the crater.

4.4. Melt inclusions

Analysis of melt inclusions in plagioclase and pyroxene crystals, as well as matrix glass, provide some insights into the petrological evolution, depth of crystallization, and degassing processes at the currently active White Island volcano. The analyzed H_2O contents of melt inclusions and calculation of the water solubility in White Island magma (Moore et al., 1998) allows calculation of the depth at which crystallization may have taken place (Fig. 5). The determined water content in melt inclusions of 0.6 ± 0.2 wt.% suggests that crystallization took place high in the magmatic system, at pressures of between 30 and 75 bars, or at depths of between about 100 and 300 m. Crystallization at shallow depths, possibly

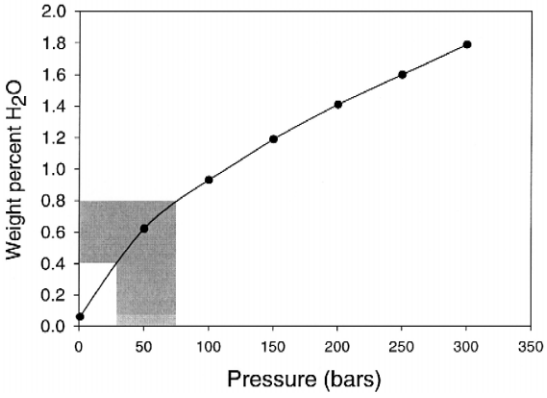

Fig. 5. Calculated H_2O solubility for a White Island dacitic glass. Calculations made following Moore et al. (1998). The shaded area shows the range of H_2O contents of White Island melt inclusions, and corresponding depths of crystallization.

triggered by degassing of H_2O and resultant polymerization of the melt, has been recognized in other open magmatic systems (Sisson and Layne, 1993; Dunbar et al., 1994). The greater Cl concentration in melt inclusions as compared to degassed matrix glass suggests that at least some fraction of the Cl was degassing from the White Island magma in the upper 300 m of the magmatic system. This is consistent with the experimentally determined results that Cl partitions strongly into an H_2O-rich vapor phase (Webster, 1992a,b). However, the SO_2 content of melt inclusions and degassed matrix glass are indistinguishable and very low, suggesting that the SO_2 being emitted from White Island degasses at depths of greater than 300 m, and by that depth, degassing of SO_2 is essentially complete. A further implication is that SO_2 degassing may be less strongly controlled by the presence of an H_2O-rich vapor phase than is Cl.

The range of melt inclusion compositions observed in White Island plagioclase suggests that many of the crystals grew initially in a more primitive melt than that with which they were erupted. As crystallization progressed, the melt evolved, becoming more enriched in SiO_2 and K_2O, and more depleted in P_2O_5, TiO_2, MgO, CaO and FeO. Similar trends have been observed in other subduction-related volcanoes (Sisson and Layne, 1993), and the magmatic evolution was attributed to H_2O exsolution triggered crystallization and resultant magmatic differentiation. In the case of White Island, the more primitive magmatic composition is typically observed in the cores of the crystals, which appear mottled or spongy in BSE imaging, possibly related to rapid crystal growth (Dunbar et al., 1994). The outer parts of the crystal are featureless. One scenario of crystal growth that could be consistent with the textural observations, as well as the chemical composition of melt inclusions would be a two-stage growth process. The initial stage of crystal growth would involve nucleation and growth of the cores of plagioclase crystals, possibly as a result of magmatic degassing (Sisson and Layne, 1993). Pyroxene crystallization could take place at the same time, and the combination of plagioclase and pyroxene crystallization could result in differentiation of the residual melt. The rims of plagioclase would then begin to grow, trapping melt inclusions of the more evolved magmatic composition. This type of compositional evolution is also observed in the crystalline matrix glass compositions, which are more evolved than the rim melt inclusions, due to further removal of pyroxene and plagioclase.

5. Conclusions

Averaging SO_2 measurements for non-eruptive plumes at White Island during a 17-year period yields a higher level of SO_2 degassing than that previously established by using two values over a 3-month period. Substituting this new value of average SO_2 emission rate into previous calculations for CO_2 flux based on CO_2/S_t ratios (Table 3) yields a higher CO_2 rate of 1550 Mg day^{-1} but is still below that observed by the direct airborne measurement of 2600 Mg day^{-1}. It is presently unclear if the lower rates are related to the difference in methodology, changes in degassing or differences in the level of activity during the measurement.

The contribution of passive degassing from the crater floor that we measured is not a significant portion of the total CO_2 flux from White Island. Since other sources of non-plume degassing such as fumaroles, the outer flanks of the crater and ocean seeps were not investigated; the magnitude of this contribution is uncertain. The CO_2 from these sources

are likely to lack the thermal buoyancy to merge with the volcanic plume and are therefore unaccounted for in any of our measurements. The total CO_2 flux from White Island, as measured by the direct airborne method, ranks it as a significant contributor of volcanic CO_2 to the atmosphere.

Results of melt inclusion studies on 1989 andesite samples suggest that crystal formation occurs at a very shallow depth (<300 m). The higher Cl and H_2O content of melt inclusions as compared to matrix glass suggests that these elements are, at least partly, degassing at depths of less than 300 m. The equally depleted SO_2 content of melt inclusions and degassed matrix glass implies that the SO_2 being emitted from White Island exsolves at depths greater than 300 m, and by that depth, degassing of SO_2 is complete. Thus, observed degassing behavior of SO_2 and CO_2 at White Island is likely to be the result of changes deeper within the system (>300 m).

Acknowledgements

Our interest and work at White Island resulted from the encouragement of the late Werner Giggenbach. Werner's love of White Island and his insatiable appetite for an understanding of magmatic degassing was the impetus for the COSPEC measurements. The airborne COSPEC and CO_2 measurements were made using aircraft from the Rotorua Aero Club (Vulcano Wunderflights), the Tauranga Aero Club and, especially, Graham Bell of Bellair in Whakatane. We thank the numerous pilots for their skill and patience in making these measurements. Access to the island for soil gas measurements was mainly by helicopter (Volcan Helicopters) and by boat (White Island Tours), so we thank Robert Fleming and Peter and Jennifer Tait for their help, guidance and attention to our needs. Our appreciation also goes to the Office of Polar Programs, NSF and the Harvard Travellers Club for their support. Thanks to Bill Rose and an anonymous reviewer for their comments which helped improve the manuscript.

References

Allard, P., 1998. Mantle-derived CO_2 budget of Mount Etna (Abstract). Eos (Trans. Am. Geophys. Union) 79, F927.

Allard, P., Carbonnelle, J., Metrich, N., Loyer, H., Zettwoog, P., 1994. Sulphur output and magma degassing budget of Stromboli volcano. Nature 368, 326–330.

Andres, R., Kasgnoc, A., 1998. A time-averaged inventory of subaerial volcanic sulfur emissions. J. Geophys. Res. 103, 25251–25261.

Brantley, S., Agustsdottir, A., Rowe, G., 1993. Crater lake reveal volcanic heat and volatile fluxes. GSA Today 3, 176–178.

Carbonnelle, J., Dajlevic, D., Bronec, J.L., Morel, P., Obert, J., Zwettwoog, P., 1985. Etna: composantes sommitales et parietales, des emissions de gas carbonique, Resulta obtenus sur la periode de 1981 a 1985. Bull. PIRPSEV-CNRS 108, 62.

Casadevall, T., Rose, W., Gerlach, T., Freenland, L., Ewert, J., Wunderman, R., Symonds, R., 1983. Gas emissions and the eruptions of Mount St. Helens through 1982. Science 221, 1383.

Casadevall, T., Neal, C., McGimsey, R., Doukas, M., Gardner, C., 1990. Emission rates of sulfur dioxide and carbon dioxide from Redoubt volcano, Alaska during the 1989–1990 eruptions. Eos (Trans. Am. Geophys. Union) 71, 1702.

Chiondini, G., Cioni, R., Guidi, M., Raco, B., Marini, L., 1998. Soil CO_2 flux measurements in volcanic and geothermal areas. Appl. Geochem. 13, 543–552.

Clark, R.H., Cole, J.W., Nairn, I.A., Wood, C.P., 1979. Magmatic eruption of White Island volcano, New Zealand, December 1976–April 1977. N. Z. J. Geol. Geophys. 22, 175–190.

Cole, J., Nairn, I., 1975. Part 22: New Zealand. Catalogue of the Active Volcanoes of the World Including Solfatara Fields. International Association of Volcanology and Chemistry of the Earth's Interior, Naples.

Cox, K.G., Bell, J.D., Pankhurst, R.J., 1979. Interpretation of Igneous Rocks. Allen & Unwin Press, London, 450 pp.

Delgado, H., Piedad-Sanchez, N., Galvan, L., Julio, P., Alvarez, J., Cardenas, L., 1998. CO_2 flux measurement at Popocatepetl volcano: II. Magnitude of emissions and significance. Eos (Trans. Am. Geophys. Union) 79, F926.

Devine, J.D., Sigurdsson, H., Davis, A.N., 1984. Estimates of sulfur and chlorine yield to the atmosphere from volcanic eruptions and potential climatic effects. J. Geophys. Res. 89, 6309–6325.

Dunbar, N.W., Cashman, K.V., Dupre, R., 1994. Crystallization processes of anorthoclase phenocrysts in the Mount Erebus magmatic system: evidence from crystal composition, crystal size distributions and volatile contents of melt inclusions. In: Kyle, P.R. (Ed.), Volcanological and Environmental Studies of Mount Erebus, Antarctica. Antarct. Res. Ser., Am. Geophys. Union 66, pp. 129–146.

Gerlach, T., Graeber, E., 1985. Volatile budget of Kilauea volcano. Nature 313, 273.

Gerlach, T., Delgado, H., McGee, K., Doukas, M., Venegas, J., Cardenas, L., 1997. Application of the LI-COR CO_2 analyzer to volcanic plumes: a case study, volcan Popocatepetl, Mexico, June 7 and 10, 1995. J. Geophys. Res. 102, 8005–8019.

Gerlach, T.M., Doukas, M., McGee, K., Kessler, R., 1998. Three-year decline of magmatic CO_2 emissions from soils of a Mammoth Mountain tree kill: Horseshoe Lake, CA, 1995–1997. Geophys. Res. Lett. 25, 1947–1950.

Giggenbach, W., 1987. Redox processes governing the chemistry of fumarolic gas discharges from White Island, New Zealand. Appl. Geochem. 2, 143–161.

Giggenbach, W., 1992. Isotopic shifts in waters from geothermal and volcanic systems along convergent plate boundaries and their origin. Earth Planet. Sci. Lett. 113, 495–510.

Giggenbach, W., 1996. Chemical composition of volcanic gases. In: Scarpa, R., Tilling, R.I. (Eds.), Monitoring and Mitigation of Volcano Hazards. Springer-Verlag, Berlin, pp. 221–256.

Giggenbach, W., Matsuo, S., 1991. Evaluation of results from Second and Third IAVCEI field workshops on volcanic gases, Mt. Usu, Japan and White Island, New Zealand. Appl. Geochem. 6, 125–141.

Giggenbach, W.F., Sheppard, D.S., 1989. Variations in the temperature and chemistry of White Island fumarole discharges 1972–1985. In: Houghton, B.F., Nairn, I.A. (Eds.), The 1976–82 Eruption Sequence at White Island Volcano (Whakaari), Bay of Plenty, New Zealand. N. Z. Geol. Surv. Bull. 103, pp. 119–126, Rotorua.

Hedenquist, J.W., Simmons, S.F., Giggenbach, W.F., Eldridge, C.S., 1993. White Island, New Zealand, volcanic–hydrothermal system represents the geochemical environment of high-sulfidation Cu and Au ore deposition. Geology 21, 731–734.

Hervig, R.L., Dunbar, N.W., Westrich, H.R., Kyle, P.R., 1989. Pre-eruptive water content of rhyolitic magmas as determined by ion microprobe analyses of melt inclusions in phenocrysts. J. Volcanol. Geotherm. Res. 36, 293–302.

Houghton, B.F., Nairn, I.A., 1989. A model for the 1976–82 phreatomagmatic and Strombolian eruption sequence at White Island volcano, New Zealand. In: Houghton, B.F., Nairn, I.A. (Eds.), The 1976–82 Eruption Sequence at White Island Volcano (Whakaari), Bay of Plenty, New Zealand. N. Z. Geol. Surv. Bull. 103, pp. 127–137, Rotorua.

Koepenick, K., Brantley, S., Thompson, J., Rowe, G., Nyblade, A., Moshy, C., 1996. Volatile emissions from the crater and flank of Oldoinyo Lengai volcano, Tanzania. J. Geophys. Res. 10, 13819–13830.

Marty, B., Giggenbach, W.F., 1990. Major and rare gases at White Island volcano, New Zealand: origin and flux of volatiles. Geophys. Res. Lett. 17, 247–250.

Moore, G., Venneman, T., Carmichael, I., 1998. An empirical model for the solubility of H_2O in magmas to 3 kilobars. Am. Mineral. 83, 36–42.

Norman, J., Garcia, R., Verma, S., 1992. Soil surface CO_2 fluxes and the carbon budget of a grassland. J. Geophys. Res. 97, 18845–18853.

O'Keeffe, M., 1994. Soil CO_2 gas concentrations and emissions at Kilauea volcano, Hawaii. MS Thesis, Earth and Environmental Science, New Mexico Institute of Mining and Technology, Socorro, NM, pp. 76.

Palais, J.M., Sigurdsson, H., 1989. Petrological evidence of volatile emissions from major historic and pre-historic volcanic eruptions. In: Berger, A., Dickenson, R. (Eds.), Contribution of Geophysics to Climate Change Studies. Geophys. Monogr., Am. Geophys. Union 15, pp. 31–53.

Roedder, E., 1984. Fluid Inclusions, Reviews in Mineralogy. Mineralogical Society of America, Washington, DC, 644 pp.

Rose, W., Chuan, R., Giggenbach, W., Kyle, P., Symonds, R., 1986. Rates of sulfur dioxide and particle emissions from White Island volcano, New Zealand, and an estimate of the total flux of major gas species. Bull. Volcanol. 48, 181–188.

Simkin, T., Siebert, L., 1994. Volcanoes of the World. Geoscience Press, Tucson, 349 pp.

Sisson, T.W., Layne, G.D., 1993. H_2O in basalt and basaltic andesite glass inclusions from four subduction-related volcanoes. Earth Planet. Sci. Lett. 117, 619–635.

Stoiber, R.E., Malinconico, L.L., Williams, S.N., 1983. Use of the correlation spectrometer at volcanoes. In: Tazieff, H., Sabroux, J.C. (Eds.), Forecasting Volcanic Events. Elsevier, Amsterdam, pp. 425–444.

Symonds, R., Reed, M., Rose, W., 1992. Origin, speciation, and fluxes of trace-element gases at Augustine volcano, Alaska: insights into magma degassing and fumarolic processes. Geochim. Cosmochim. Acta 56, 633–657.

Tedesco, D., Toutain, J., 1991. Chemistry and emission rate of volatiles from White Island volcano (New Zealand). Geophys. Res. Lett. 18, 113–116.

Varley, N., 1998. Diffuse degassing of Popocatepetl volcano, Mexico. Eos (Trans. Am. Geophys. Union) 79, F927.

Wardell, L., Kyle, P., 1999. Carbon dioxide emissions from Mt. Erebus, Antarctica. Ant. J. U.S. in press.

Watson, E.B., 1976. Glass inclusions as samples of early magmatic liquid: determinative method and application to a South Atlantic basalt. J. Volcanol. Geotherm. Res. 1, 73–84.

Webster, J.D., 1992a. Fluid–melt interactions involving Cl-rich granites: experimental study from 2 to 8 kbar. Geochim. Cosmochim. Acta 56, 659–678.

Webster, J.D., 1992b. Water solubility and chlorine partitioning in Cl-rich granitic systems: effects of melt composition at 2 kbar and 800°C. Geochim. Cosmochim. Acta 56, 679–687.